Acta Pharmaceutica Sinica B 2022;12(7):3177–3186

Chinese Pharmaceutical Association
Institute of Materia Medica, Chinese Academy of Medical Sciences

Acta Pharmaceutica Sinica B

www.elsevier.com/locate/apsb
www.sciencedirect.com

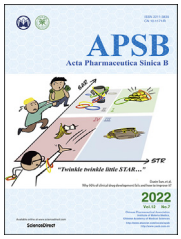

SHORT COMMUNICATION

Generation of αGal-enhanced bifunctional tumor vaccine

Jian He[a,†], Yu Huo[a,†], Zhikun Zhang[a,†], Yiqun Luo[a], Xiuli Liu[a], Qiaoying Chen[a], Pan Wu[a], Wei Shi[b], Tao Wu[c], Chao Tang[a], Huixue Wang[a], Lan Li[a], Xiyu Liu[a], Yong Huang[a], Yongxiang Zhao[a], Lu Gan[a,*], Bing Wang[d,*], Liping Zhong[a,*]

[a]*National Center for International Research of Biotargeting Theranostics, Guangxi Key Laboratory of Biotargeting Theranostics, Collaborative Innovation Center for Targeting Tumor Diagnosis and Therapy, Guangxi Talent Highland of Biotargeting Theranostics, Guangxi Medical University, Nanning 530021, China*
[b]*The First Affiliated Hospital, Guangxi University of Chinese Medicine, Nanning 530023, China*
[c]*The First People's Hospital of Changde City, Changde 415003, China*
[d]*Department of Spine Surgery, the Second Xiangya Hospital of Central South University, Changsha 410011, China*

Received 7 December 2021; received in revised form 2 February 2022; accepted 11 February 2022

KEY WORDS

αGal;
Endoglin;
Dendritic cells;
Fusion cells;
Hepatocellular carcinoma;
Tumor neovascular endothelial cells;
Cytotoxic T lymphocytes;
Immunotherapy

Abstract Hepatocellular carcinoma (HCC) is a common malignant tumor with poor prognosis and high mortality. In this study, we demonstrated a novel vaccine targeting HCC and tumor neovascular endothelial cells by fusing recombinant MHCC97H cells expressing porcine α-1,3-galactose epitopes (αGal) and endorphin extracellular domains (END) with dendritic cells (DCs) from healthy volunteers. END^{+}/Gal^{+}-MHCC97H/DC fusion cells induced cytotoxic T lymphocytes (CTLs) and secretion of interferon-gamma (IFN-γ). CTLs targeted cells expressing αGal and END and tumor angiogenesis. The fused cell vaccine can effectively inhibit tumor growth and prolong the survival time of human hepatoma mice, indicating the high clinical potential of this new cell based vaccine.

*Corresponding authors.
E-mail addresses: zhong_liping@163.com (Liping Zhong), wbxyeyy@csu.edu.cn (Bing Wang), g_lganlu@163.com (Lu Gan).
†These authors made equal contributions to this work.

Peer review under responsibility of Chinese Pharmaceutical Association and Institute of Materia Medica, Chinese Academy of Medical Sciences.

https://doi.org/10.1016/j.apsb.2022.03.002

1. Introduction

Hepatocellular carcinoma (HCC) is a highly malignant cancer, ranking second in cancer-related deaths[1]. Currently, hepatectomy is the only curative treatment. However, recurrence is common due to failure to completely remove the tumor tissue and unresectable advanced tumors. Non-surgical treatments for HCC such as radiation therapy or chemotherapy are generally ineffective and often cause serious side effects[2,3].

To tackle these challenges, T cell-based adoptive immunotherapy emerged as a promising alternative strategy. Immunotherapy involves extracting specific cell populations from a patient, activating and expanding them *in vitro*, and then transferring them back into the patient to elicit antitumor immune responses[4,5]. Dendritic cells (DCs) are specialized antigen presenting cells, which can effectively induce the activity of T cells. Therefore, fusion of DCs with tumor cells can activate cytotoxic T lymphocytes (CTLs) to trigger effective tumor-specific immune response[6−8]. The high efficiency and specificity of this CTL-mediated cytotoxicity demonstrates the possibility of developing an effective cancer vaccine[9−11].

We conceived that expressing alpha-1,3-galactosyl epitope(αGal) on tumor cells could enhance the vaccination ability of tumor/DC fusion cells. Due to lack of α-1,3-galactosyltransferase (α1,3 GT), cell surface of human, ape and old-world monkey do not express αGal antigen, and there are natural antibodies in serum of these species[12]. Engineering tumor cells to express αGal on their surface enables interaction with anti-αGal antibodies and subsequent recruitment of circulating complement factors to attack tumor cells, causing a cascade of amplified immune responses[13]. In addition to antibody-mediated antitumor activity, αGal also promotes T cell activation and secretion of cytokines such as TNF-α, IFN-γ, granzyme B, and IP-10[14].

Type one membrane glycoprotein endoglin (END) is mainly expressed on tumor neovascular endothelial cells, but rarely expressed in normal endothelial cells. It plays a vital role in the process of tumor vascular proliferation, which is closely related to tumor proliferation and invasion[15]. It is recognized as a cancer-specific marker molecule for tumor neovascular endothelial cells[15,16]. Inhibiting END with antibodies or blocking its expression has shown therapeutic potential in animal studies[17−19]. Nevertheless, it has yet to be exploited as a targeted antigen in adoptive immunotherapy. We hypothesized that expressing END on tumor/DC fusion cells could create a vaccine against neovascular endothelial cells in tumors.

In this manuscript we reported a new adoptive immunotherapy approach that simultaneously targets HCC and tumor neovascular endothelial cells. DCs fused with MHCC97H cells expressing both αGal and END to activate CTL, which produced cytotoxic effects on HCC cells and tumor neovascular endothelial cells. Human hepatocellular carcinoma developed by MHCC97H cell line, with strong invasiveness and rich blood vessels, was selected as the tumor treatment model in this study. We demonstrated the high efficiency and specificity of this CTL-mediated vaccine both *in vitro* and *in vivo*. The outstanding therapeutic effects were attributed to the fact that these fusion cells simultaneously presented entire HCC-specific antigens together with αGal and END to T cells and they could trigger potent and multifaceted immune responses to suppress tumor.

2. Material and methods

2.1. Cells and animals

The following cell lines were purchased from the American Type Culture Collection (ATCC, Manassas, VA, USA): A549 human lung adenocarcinoma epithelial cells, MHCC97H human hepatocellular carcinoma cells, and human umbilical vein endothelial cells (HUVEC). A549 cells were cultured in complete RPMI-1640 medium (GIBCO, Thermo Fisher Scientific, Waltham, MA, USA) containing 10% fetal bovine serum (GIBCO). MHCC97H cells stably expressing α1,3 GT or/and END and MHCC97H cells stably transduced with empty pLVX-Puro vector were generated using GenScript (Nanjing, China) and maintained in minimal essential medium (MEM; GIBCO) supplemented with 10% FBS, 100 U/mL penicillin/streptomycin, and 0.35 μg/mL puromycin (Sigma−Aldrich, St. Louis, MO, USA). HUVECs expressing endogenous END were cultured in complete RPMI-1640 media containing 10% FBS. Cells were cytogenetically tested and authenticated before freezing. Each vial of frozen cells was thawed and maintained for a maximum of 10 weeks.

Specific pathogen-free, athymic nude BALB/c mice aged 4 weeks and weighing 16−18 g were provided by the Experimental Animal Center in Guangxi Medical University (Nanning, China). T cells were purified from peripheral blood mononuclear cells (PBMCs) isolated from 15 healthy human volunteers (aged 23−26, eight males, seven females). All human and animal experiments were performed according to the guidelines of the Federation of European Laboratory Animal Science Association, and all protocols approved by the Animal and Human Ethics Committee of Guangxi Medical University (Nanning, China).

2.2. Construction and stable transduction of MHCC97H cells expressing α1,3 GT or/and END

Complementary DNAs encoding α1,3 GT or/and END were cloned into the lentiviral pLVX-Puro vectors. The three constructs were co-transfected together with Lenti-X HTX packaging plasmid (Clontech Laboratories, Mountain View, CA, USA) into Lenti-X 293T cells to generate virus stock for transducing MHCC97H cells. Stably transduced MHCC97H cells were selected by puromycin resistance and respectively named Gal^+-MHCC97H, END^+-MHCC97H and END^+/Gal^+-MHCC97H. The empty pLVX-puro lentiviral expression vector was used as control (pLVX-vector). Western blot was used to detect the expression of protein END. Expression of fusion protein α1,3 GT-END was assayed by immunofluorescence.

2.3. Isolation and generation of human T lymphocytes and DCs

PBMCs were isolated from fresh peripheral blood at room temperature using human lymphocyte separation medium (Dakewe Biotech, Shenzhen, China). After washing 3 times in RPMI-1640 (20 °C, 250 × *g*, 10 min), PBMCs were resuspended at a density of 1×10^7 cells/mL and seeded in a Corning Costar 6-well plate (Sigma−Aldrich). After incubating for 2 h, cells were collected and seeded in a new 6-well plate, and 20 U/mL of recombinant human interleukin-2 (rhIL-2) was added. T cells were then purified by filtering through a nylon wool column. The original 6-well plate that contained adherent

cells was filled with two mL complete medium supplemented with 1000 U/mL of recombinant human granulocyte/macrophage colony-stimulating factor (rhGM-CSF) and 500 U/mL of rhIL-4. On Day 5, rhGM-CSF was reduced by half and 25 ng/mL of tumor necrosis factor-α (TNF-α) was added to the cells. All cytokines were purchased from R&D Systems (Minneapolis, MN, USA).

2.4. Preparation of MHCC97H/DC fusion cells

DCs cultured for 7 days were mixed in a 2:1 ratio with MHCC97H cells, MHCC97H[pLVX-Puro], END$^+$-MHCC97H, Gal$^+$-MHCC97H or END$^+$/Gal$^+$-MHCC97H that had been treated with 30-Gy radiation. The mixture in phosphate-buffered saline (PBS) was centrifuged at 200 × *g* for 10 min; the supernatant was removed, and polyethylene glycol (PEG; Sigma−Aldrich) was added to the cells, then incubated at 37 °C in a water bath for 5 min. RPMI-1640 medium was added to stop the reaction. Cells were centrifuged again, washed twice with PBS, and resuspended in RPMI-1640 supplemented with 10% FBS, 500 U/mL rhGM-CSF, and 500 U/mL rhIL-4. This suspension was left standing for 24 h at 37 °C, after which the cells were considered to be MHCC97H/DC fusion cells.

2.5. Fluorescence detection

MHCC97H cells, MHCC97H[pLVX-Puro] cells, END$^+$-MHCC97H cells, Gal$^+$-MHCC97H cells and END$^+$/Gal$^+$-MHCC97H cells (5×10^5 cells/type) were incubated at 4 °C for 3 h with 10 μg/mL of Alexa Fluor 647-conjugated isolectin *Griffonia simplicifolia*-IB4 (GS-IB4; Invitrogen, Thermo Fisher Scientific, Waltham, MA, USA). The α1,3 GT enzyme encoded by the gene transduced them into MHCC97H cells that produced αGal, which bound the isolectin GS-IB4. FITC-conjugated anti human END antibody bound the expression of END on cells. Fluorescently labeled cells were detected using laser scanning confocal microscope (Nikon, Tokyo, Japan) and flow cytometry (Beckman Coulter Epics XL-MCL, Danvers, MA, USA). The expression of CD83, CD86, HLA-DR and HLA-ABC on the surface of DCs was detected by flow cytometry. Data was analyzed with Kaluza Analysis Software (Ashland, OR, USA).

2.6. Western blot analysis of fusion cells

END$^+$/Gal$^+$-MHCC97H, Gal$^+$-MHCC97H, END$^+$-MHCC97H, and MHCC97H[pLVX-Puro] cells were disrupted in RIPA lysis buffer (Beyotime Biotechnology, Shanghai, China). Total protein concentration was determined using BCA Protein Quantification Kit (Beyotime Biotechnology). Equal amounts of protein from different cells were separated by 10% sodium dodecyl sulfate-polyacrylamide gel electrophoresis and transferred onto a nitrocellulose membrane. Nonspecific binding was blocked using 5% (*w*/*v*) non-fat dry milk in Tris-buffered saline with 0.1% Tween-20 (TBST). The membrane was incubated at 4 °C overnight with a mouse anti-human END monoclonal antibody (Abcam, Cambridge, UK). After washing 3 times with TBS-T, the membrane was incubated with a horseradish peroxidase (HRP)-labeled rabbit anti-mouse secondary antibody (ZSGB-Bio, Beijing, China). Protein bands were visualized using the diaminobenzidine (DAB) kit (SolarBio, Beijing, China).

2.7. Cytotoxicity of fusion cell-stimulated CTLs

Cytotoxicity of fusion cell-stimulated CTLs was analyzed by radioactive ^{51}Cr release assays. T lymphocytes were incubated with different types of fusion cells for 7 days. 293T, A549, HUVEC, MHCC97H, END$^+$-MHCC97H, Gal$^+$-MHCC97H and END$^+$/Gal$^+$-MHCC97H cells were labeled with ^{51}Cr and seeded into 96-well plates (1×10^4 cells/well). Stimulated T lymphocytes were added to the wells at effector/target (E/T) ratios of 3:1, 10:1, or 30:1. ^{51}Cr release was counted on a γ radiation counter and measured in counts per minute (cpm). Maximum release was determined from supernatants of cells that were lysed by addition of 5% Triton X-100. Spontaneous release was determined from target cells incubated without added effector cells. Wells were incubated for 5 h, and cpm were measured in the culture supernatant fraction using a γ radiation counter. The percent specific cytotoxicity was calculated using Eq. (1):

$$\text{Cytotoxicity (\%)} = [(\text{Experimental release} - \text{Spontaneous release}) / (\text{Maximum release} - \text{Spontaneous release})] \times 100 \quad (1)$$

2.8. Assay of interleukin and interferon by fusion cells

The five types of MHCC97H/DC fusion cells were seeded at a density of 1×10^5 cells/mL and cultured for 48 h before collecting the supernatant. Secreted IL-12p70 was measured using an ELISA kit purchased from R&D Systems. Human IFN-γ was assayed using ELISPOT as follows: Fusion cells were mixed with T cells at a ratio of 1:10 and cultured in ELISPOT plates precoated with human IFN-γ antibody (Dakewe Biotech, Shenzhen, China). After 7 days, cells were disrupted and a biotin-labeled detection antibody was added, followed by HRP-conjugated streptavidin. Spots were visualized and analyzed using a CTL-ImmunoSpot Analyzer (Cellular Technology, Shaker Heights, OH, USA).

2.9. T cell-based adoptive transfer

BALB/c nude male mice were randomly divided into six groups ($n = 20$ in each group). MHCC97H cells in the log growth phase were collected and resuspended at a density of 2×10^6 cells/mL, and 100 μL of cell suspension was subcutaneously injected into the right axilla of each mouse. T cells previously stimulated by mixing at a ratio of one fusion cell per 10 T cells for 7 days and then filtering through nylon wool. On Days 5, 12, 19, 26, and 33, mice were injected in the tail veins with stimulated T cells (5×10^6/mouse). Control mice were injected MHCC97H cells instead of stimulated T cells. On Day 33 after the mice had received five adoptive transfers, five mice from each group were sacrificed, and tumor samples were taken for immunohistochemical analysis. Tumor volumes (length × width^2 × 0.5) was measured every 5 days. Mice were followed for 90 days or until death in order to calculate the survival rate.

2.10. Immunohistochemistry of tumor sections

The frequency of apoptotic cells in tumor tissue sections were determined by TUNEL detection kit (Roche, Swiss). All images were screened under a fluorescence microscope (Nikon, Tokyo, Japan). Paraffin sections were cut from tumor tissue blocks and stained with a mouse monoclonal antibody against human proliferating cell nuclear antigen (PCNA) following manufacturer's instructions (Boster, Wuhan, China). Expression of CD31

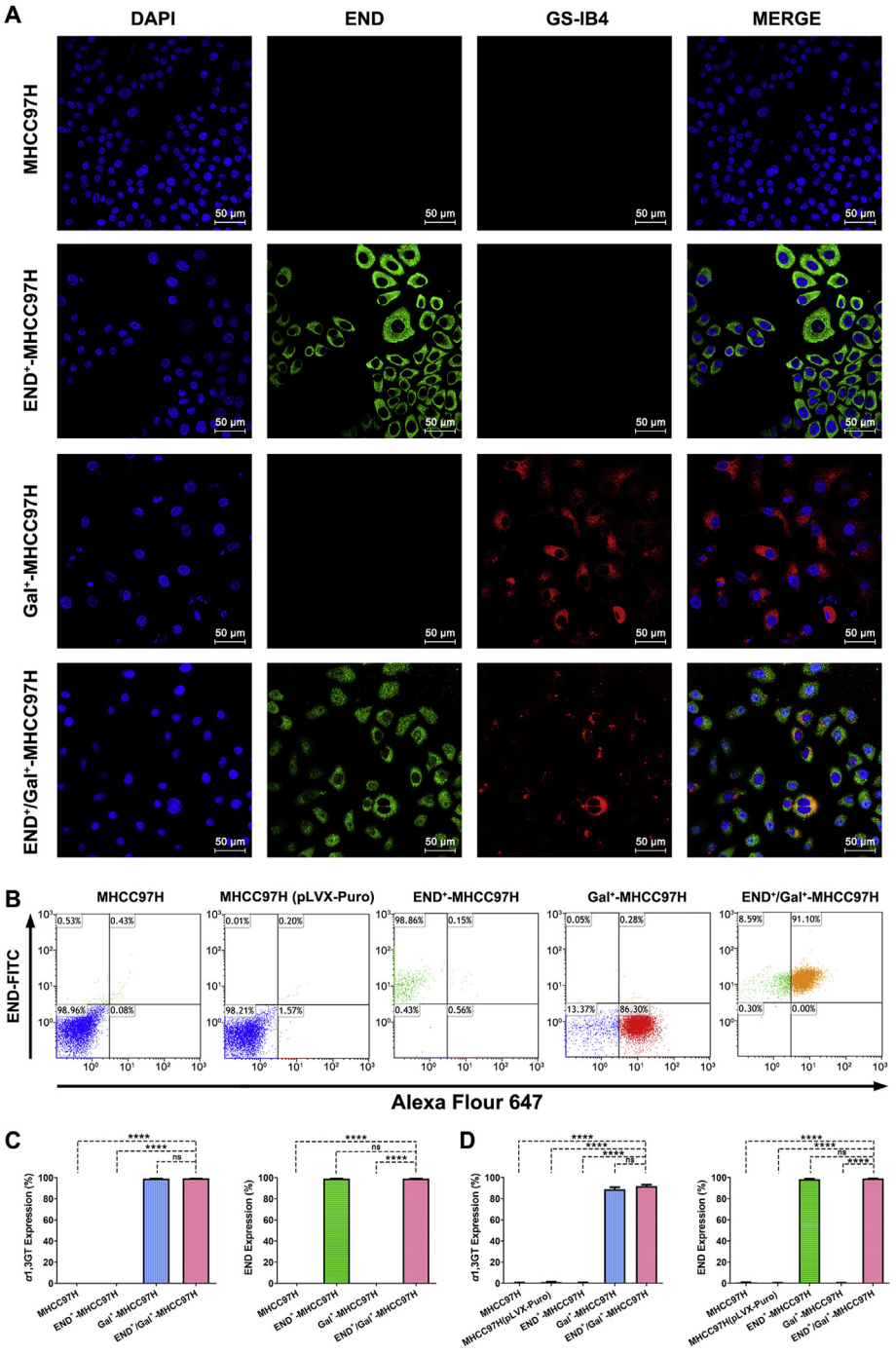

Figure 1 Generation of END$^+$-MHCC97H, Gal$^+$-MHCC97H and END$^+$/Gal$^+$-MHCC97H cells. (A) Immunofluorescence was used to detect the expression of END, α1,3 GT, and α1,3 GT-END in MHCC97H cells. END$^+$-MHCC97H cells were bound by FITC-conjugated anti-human END antibody; Gal$^+$-MHCC97H cells were stained by Alexa Fluor 647-conjugated isolectin GS-IB4 lectin; END$^+$/Gal$^+$-MHCC97H cells were labeled by both fluorescent dye. MHCC97H cells were used as negative controls. Red: GS-IB4; Green: anti-human END antibody; Blue: nucleus. (Original magnification, 400 ×; Scale bar, 50 μm). (B) Expression of α1,3 GT and END in MHCC97H, MHCC97H (pLVX-Puro), END$^+$-MHCC97H, Gal$^+$-MHCC97H and END$^+$/Gal$^+$-MHCC97H cells were assessed by flow cytometry. Quantitative analysis for immunofluorescence (C) and flow cytometry (D). ****$P < 0.0001$, ns stands for no difference. Data are representative of at least three individual experiments and are presented as mean ± SD.

was detected in frozen sections of tumor tissues as follows: frozen sections were fixed in cold acetone for 10 min, blocked using 5% bovine serum albumin at 37 °C for 30 min, and incubated at 4 °C overnight with a rat monoclonal antibody against mouse CD31 (1:400; Abcam, Shanghai, China). Sections were then stained with a horseradish peroxidase-conjugated rabbit anti-rat secondary antibody (ZSGB-Bio, Signal was developed using a DAB detection kit (ZSGB-Bio, Beijing, China).

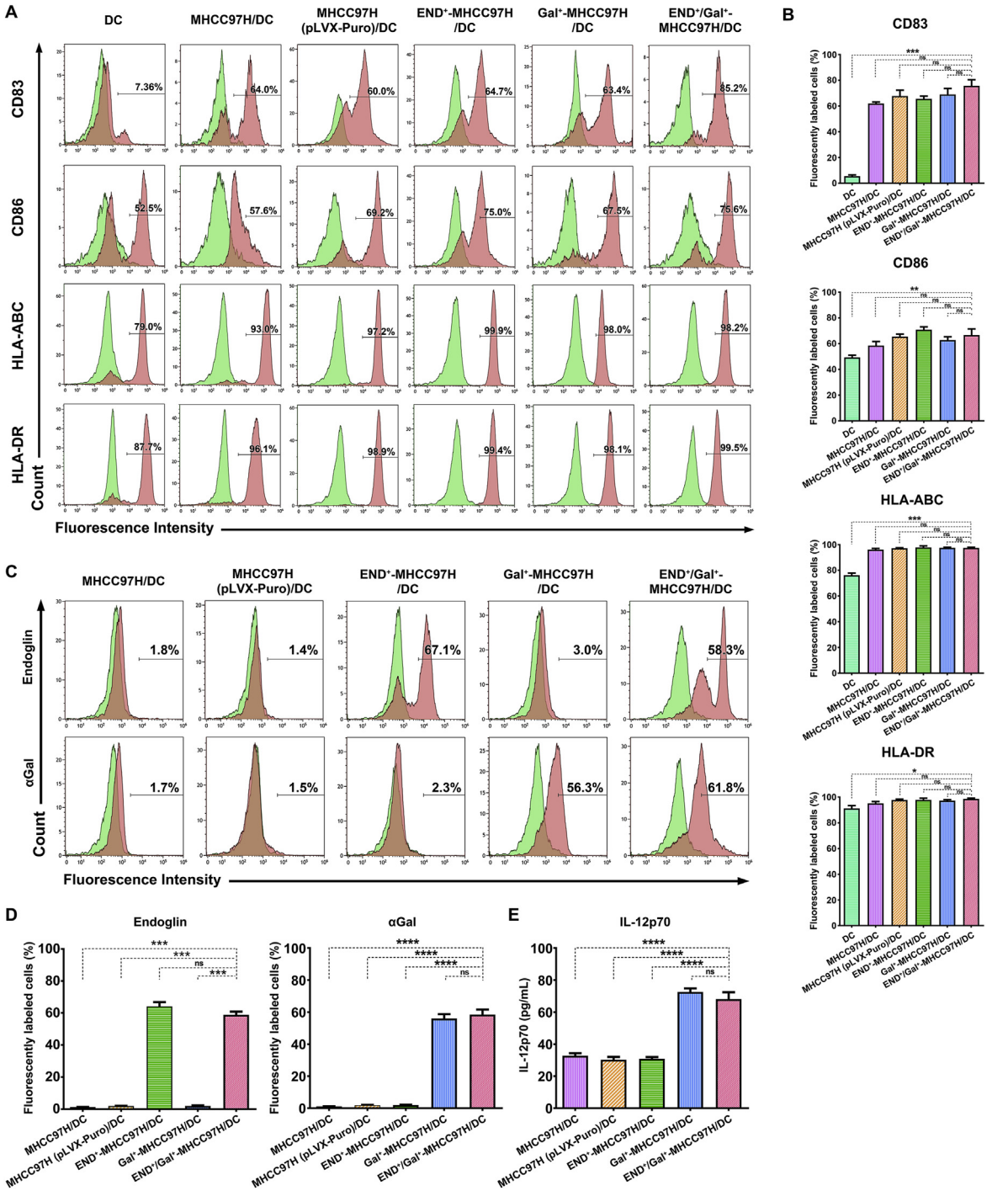

Figure 2 Detection of cell surface markers and production of IL-12p70 by five types of MHCC97H/DC fusion cells. Flow cytometry was used to assess the expression of cell surface markers, including CD83, CD86, HLA-ABC, HLA-DR, END and αGal. Flow cytometry analysis of CD83, CD86, HLA-ABC, and HLA-DR (A) and quantitative analysis (B). (C) Flow cytometry analysis of END as well as αGal. (D) Quantitative analysis. (E) ELISA was used to assay levels of IL-12p70 secreted after 48 h culture. $^{*}P < 0.05$, $^{**}P < 0.01$, $^{***}P < 0.001$, $^{****}P < 0.0001$, ns stands for no difference. Data show mean ± SD and individual values from three independent experiments.

2.11. Bioinformatics analysis

Gene_DE module was used to study the differential expression between tumor and adjacent normal tissues for any gene of interest across all TCGA tumor. Distributions of END gene expression levels were displayed using box plots. The statistical significance computed by the Wilcoxon test was annotated by the number of stars. ($^{*}P < 0.05$; $^{**}P < 0.01$; $^{***}P < 0.001$). Then, definitions and outcomes of overall survival (OS) were extracted from the TCGA-Clinical Data ($n = 364$). Datasets assigned to high- and low-risk groups based on the risk score.

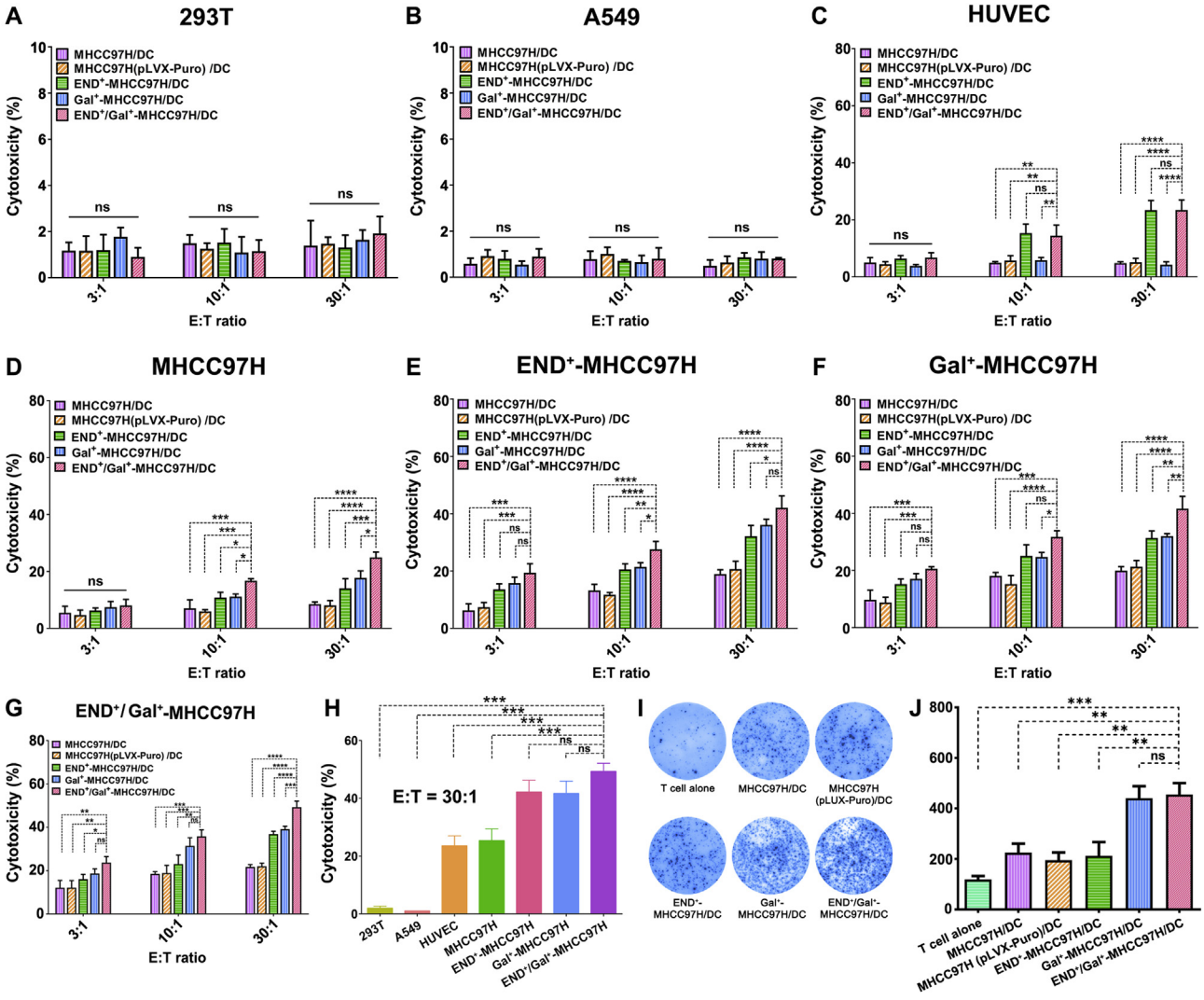

Figure 3 Cytotoxicity of T cells against ^{51}Cr-labeled target cells after induction by different types of MHCC97H/DC fusion cells, at different ratios of effector cells (T cells) to target cells (E:T). Target cells were (A) 293T, (B) A549, (C) HUVEC, (D) MHCC97H, (E) END$^+$-MHCC97H, (F) Gal$^+$-MHCC97H, and (G) END$^+$/Gal$^+$-MHCC97H/DC. (H) Cytotoxicity of T cells stimulated by END$^+$/Gal$^+$-MHCC97H/DC fusion cells was compared for other indicated target cells. In all cases, the ratio of T cells to target cells was 30:1. Measurement of IFN-γ-producing T cells following 7-day co-culture of with different types of MHCC97H/DC fusion cells. (I) Representative ELISPOT results. (J) Average numbers of IFN-γ-producing T cells per sample of 3×10^5 T cells. Spot numbers of Gal$^+$-MHCC97H/DC and END$^+$/Gal$^+$-MHCC97H/DC fusion cells were significantly greater than that of other fusion cell types. $^{**}P < 0.01$, $^{***}P < 0.001$, $^{****}P < 0.0001$, ns stands for no difference. Data are representative of at least three individual experiments and are presented as mean ± SD.

2.12. Statistical analysis

All data were analyzed using GraphPad Prism 8.0 (La Jolla, CA, USA). Differences between two groups were assessed for significance using one-way ANOVA, while differences between more than two groups were assessed using Bonferroni's multiple-comparison procedures. Survival rates were determined using Kaplan−Meier survival curves, which were compared between groups using the log-rank test. $P < 0.05$ was considered statistically significant.

3. Results

3.1. Generation of MHCC97H cells stably expressing α1,3 GT/END fusion protein

Fusion plasmid consisting of α1,3 GT and END extracellular domain were subcloned downstream of the tumor-specific hTERT promoter in a lentiviral vector and stably transduced into MHCC97H cells (Supporting Information Fig. S1A). In parallel, fusion plasmids of only α1,3 GT or END were also transduced into MHCC97H cells for comparison. α1,3 GT-END fusion plasmid was predicted to have a molecular weight of 100 kDa, comprised of α1,3 GT (35 kDa), and END extracellular domain (65 kDa). Western blot analysis confirmed expression of the desired fusion proteins in END$^+$/Gal$^+$-MHCC97H (Fig. S1B). In addition, the proper function of α1,3 GT was confirmed by detecting production of αGal, which bound Alexa Fluor 647-conjugated glycoprotein GS-IB4. The expression of END on cells was detected by FITC-conjugated anti human END antibody. As expected, END$^+$/Gal$^+$-MHCC97H cells were labeled by red and green, Gal$^+$-MHCC97H cells were labeled by red, END$^+$-MHCC97H were labeled by green; whereas, MHCC97H (pLVX-Puro) and MHCC97H cells were not labeled (Fig. 1A−D). These results indicated that a stable expression of

the exogenous fusion protein α1,3 GT-END was successfully achieved.

3.2. *Fusions between DC and END$^+$/Gal$^+$-MHCC97H cells*

All five types of fusion cells possessed the DC markers including CD83 and CD86, HLA-ABC, and HLA-DR (Fig. 2A and B). They had the characteristics of typical mature DCs, and expressed α1,3 GT, or/and END (Fig. 2C and D). The successful fusion between green fluorescence labelled DCs and red fluorescence labelled MHCC97H cells was confirmed by fluorescence microscope (Supporting Information Fig. S2).

3.3. *END$^+$/Gal$^+$-MHCC97H/DC fusion cells secrete more IL-12p70*

Culturing the fusion cells for 48 h and then assaying production of IL-12p70 showed that END$^+$/Gal$^+$-MHCC97H/DC and Gal$^+$-MHCC97H/DC fusion cells secreted significantly more of this interleukin than END$^+$-MHCC97H/DC, DC/MHCC97H (pLVX-Puro), or MHCC97H/DC fusion cells (Fig. 2E, $P < 0.001$). This was expected, as αGal is known to enhance IL-12p70 production. IL-12p70 is an important cytokine that mediates cellular immunity. In addition to increasing the killing activity of NK/LAK, IL-12P70 can also stimulate CTLs to exert anti-tumor effects[20].

3.4. *END$^+$/Gal$^+$-MHCC97H/DC fusion cells stimulate T cell-mediated cytotoxic response and IFN-γ production from T cells*

T cells induced by any of the five fusion cell types showed minimal cytotoxicity against 293T cells or A549 cells (Fig. 3A and B), suggesting their high therapeutic specificity. T cells activated by END$^+$/Gal$^+$-MHCC97H/DC or Gal$^+$-MHCC97H/DC fusion cells showed significantly greater cytotoxicity against MHCC97H cells than T cells activated by other fusion cell types. On the other hand, T cells activated by fusion cells expressing the extracellular domain of END showed greater toxicity against HUVEC cells (Fig. 3C and D). Similar to MHCC97H Cells, END$^+$-MHCC97H cells, Gal$^+$-MHCC97H cells, and END$^+$/Gal$^+$-MHCC97H cells were able to exert cytotoxic effects (Fig. 3E–G). END$^+$/Gal$^+$-MHCC97H/DC fusion cells stimulated CTLs against both tumor cells and tumor neovascular endothelial cells. In other words, they not only induced direct killing of tumor cells, but also cut the nutrient supply to tumor tissue. In contrast, 293T cells and A549 cells did not express END (Supporting Information Fig. S3). At a ratio of T cells to target cells 30:1, T cells primed by END$^+$/Gal$^+$-MHCC97H/DC fusion cells showed much greater cytoxicity against MHCC97H, END$^+$-MHCC97H, Gal$^+$-MHCC97H, END$^+$/Gal$^+$-MHCC97H and HUVEC cells, than against 293T and A549 cells (Fig. 3H).

IFN-γ can inhibit tumor cell proliferation by regulating the expression of a variety of proliferation-related genes, blocking the tumor cell cycle, and promoting tumor cell apoptosis. It can up-regulate the activity of various immune cells such as DCs, macrophages, B cells, and T cells. Co-culturing T cells with fusion cells and then measuring the number of T cells producing IFN-γ showed that the numbers were significantly higher with END$^+$/Gal$^+$-MHCC97H/DC or Gal$^+$-MHCC97H/DC fusion cells than with other fusion cell types (Fig. 3I and J). It suggested that αGal stimulated T cells to secrete this cytokine.

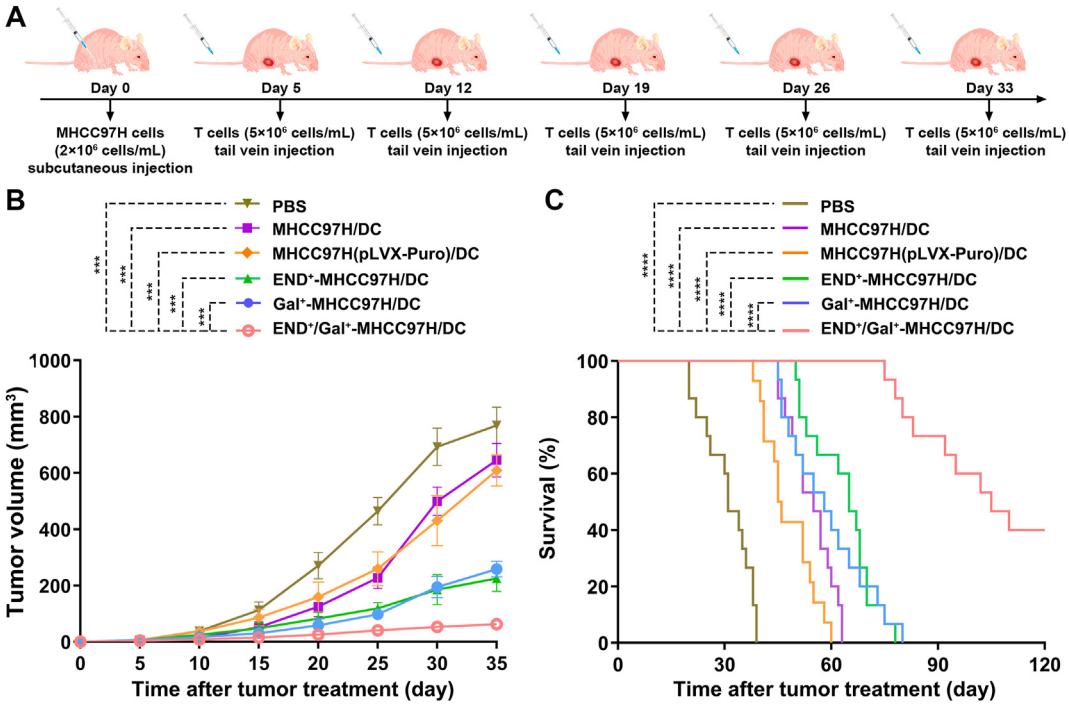

Figure 4 Antitumor effects of T cells induced by different types of MHCC97H/DC fusion cells. (A) Mice injected with MHCC97H cells (2×10^6 cells/mouse on Day 0) were treated with stimulated T cells once a week (from Day 5 to Day 33). (B) Tumor volume was measured every 5 days from Day 5 to Day 35. Tumors were significantly smaller in mice treated with T cells primed by END$^+$/Gal$^+$-MHCC97H/DC fusion cells than in mice treated with T cells primed by other types of fusion cells. ***$P < 0.001$ (by Day 35). (C) Kaplan–Meier survival curves of hepatoma-bearing nude mice ($n = 15$ in each group). Curves were compared using the log-rank test. ****$P < 0.0001$.

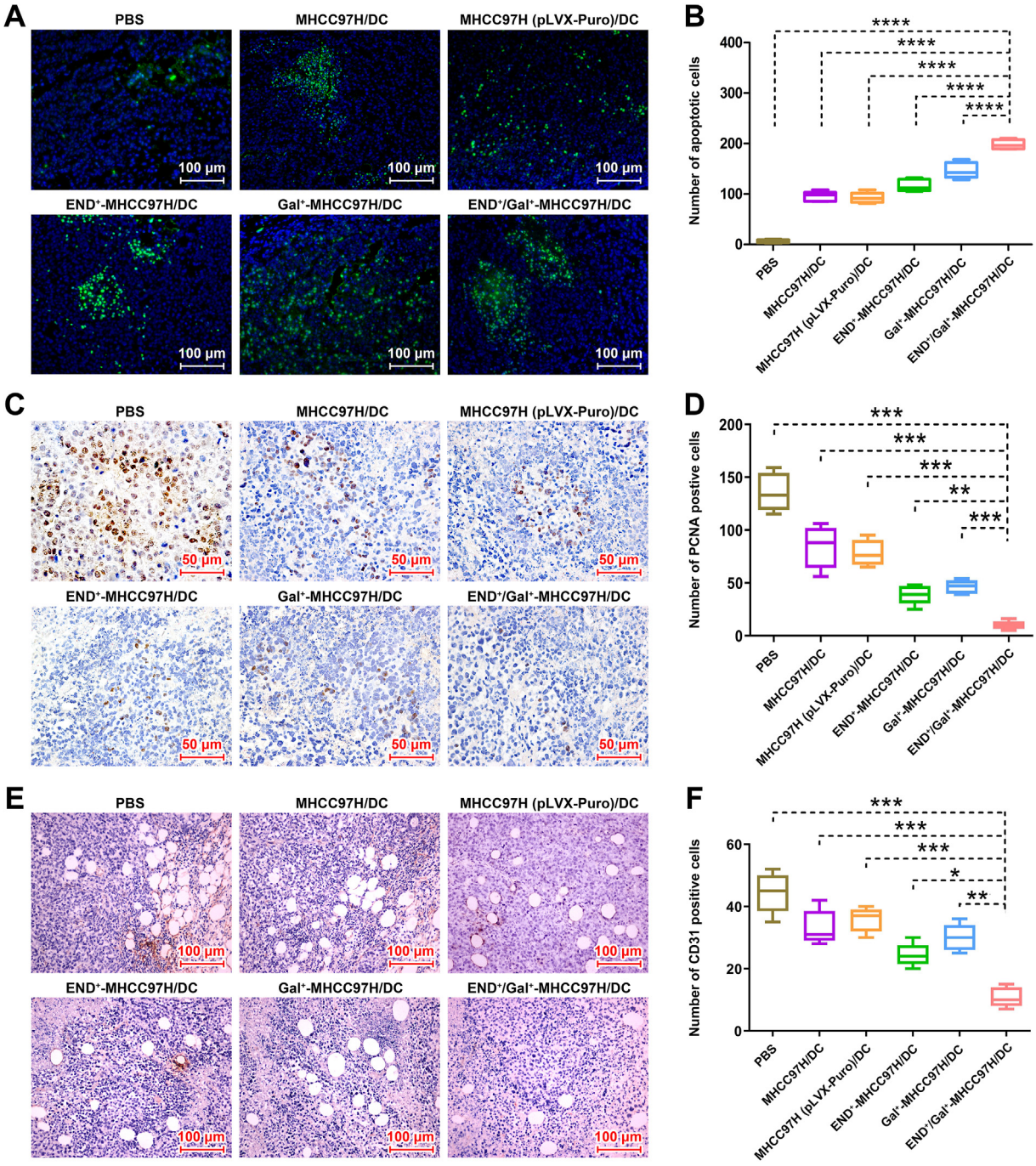

Figure 5 Mice had been injected with PBS or T cells stimulated by one of the following types of fusion cells: MHCC97H/DC, MHCC97H (pLVX-Puro)/DC, END$^+$-MHCC97H/DC, Gal$^+$-MHCC97H/DC, END$^+$/Gal$^+$-MHCC97H/DC. T cells stimulated by END$^+$/Gal$^+$-MHCC97H/DC fusion cells increased tumor cell apoptosis and inhibited their proliferation and microvessel formation in hepatoma-bearing nude mice. Cells apoptosis in tumor tissues of mice that received different treatments were detected by TUNEL. (A) TUNEL staining in the tumor tissues of mice that received different treatments (Original magnification, 200 ×; scale bar, 100 μm). (B) The mean and standard deviation of TUNEL staining in each group. (C) PCNA staining in tumor tissues of mice that received different treatments (Original magnification, 400 ×; scale bar, 50 μm). (D) PCNA-positive cells were counted in five randomly selected fields of tumor thin sections. Quantitative analysis for average numbers of positive cells. (E) Expression of CD31 in tumor tissues of mice that received different treatments (Original magnification, 200 ×; scale bar, 100 μm). (F) CD31-positive microvessels were counted in five randomly selected fields of tumor thin sections. Quantitative analysis for average numbers of microvessels. *$P < 0.05$, **$P < 0.01$, ***$P < 0.001$. Data are representative of at least three individual experiments and are presented as mean ± SD.

3.5. *Vaccines based on END$^+$/Gal$^+$-MHCC97H/DC fusion cell inhibit tumor growth in nude mice bearing human and prolong survival*

The fusion cell-stimulated T cells (5×10^6) were injected into the tumor-bearing mice through their tail veins. The control group was injected with 100 μL PBS (Fig. 4A). Average hepatoma volume was smaller in mice receiving T cells stimulated by END$^+$/Gal$^+$-MHCC97H/DC fusion cells than in mice receiving T cells stimulated by Gal$^+$-MHCC97H/DC or END$^+$-MHCC97H/DC fusion cells (Fig. 4B), implying the synergistic effects of Gal and END. By Day 90, 11 of 15 mice (73%) that had received T cells stimulated with END$^+$/Gal$^+$-MHCC97H/DC fusion cells were alive, while all mice in other treatment groups had died (Fig. 4C). The TUNEL assay revealed that END$^+$/Gal$^+$-MHCC97H/DC fusion cells caused a significant increase in the number of apoptotic cells in tumor tissues, as compared to other groups (Fig. 5A and B). PCNA is an indicator of cell proliferation. CD31 can be used to estimate tumor microvessel density and as an indicator of tumor microangiogenesis. Immunohistochemistry of tumor sections indicated significantly fewer PCNA or CD31 positive cells in mice that received T cells stimulated by END$^+$/Gal$^+$-MHCC97H/DC fusion cells than other groups (Fig. 5C−F). Importantly, we found no toxicity in heart, liver, lung or kidney tissue of mice injected with stimulated T cells by END$^+$/Gal$^+$-MHCC97H/DC (Supporting Information Fig. S4).

4. Discussion

In this study, we demonstrated that genetically engineered END$^+$/Gal$^+$-MHCC97H/DC fusion cells as a vaccine can stimulate CTLs to suppress tumor growth and increase survival of mice bearing human HCC. The remarkable efficacy is attributable to synergistic immune-triggering effects from αGal and END co-expressed on fusion cells.

Tumor cell vaccine expressing αGal requires *in vivo* binding of anti-αGal antibodies to DCs in the circulation in order to present tumor antigens to T cells[21]. Therefore, since the amount of DCs in circulation is destitute, the number of T cells being activated was insufficient. Consequently, the antitumor effects of such vaccine would be limited. In comparison, our method was not restricted by the number of circulating DCs, because the αGal expressed by fusion cells maybe promote DCs to efficiently recognize known and unknown tumor antigens and present them to T cells. In addition, αGal, a heterologous antigen, strongly stimulates the rapid proliferation of T cells. END$^+$/Gal$^+$- MHCC97H/DC and Gal$^+$-MHCC97H/DC fusion cells could abundantly secrete IL-12p70 and promote CTLs to produce IFN-γ. It was speculated that αGal played an important role in the promoting maturation of DCs, thereby promoting the presentation of antigens by DCs. Besides, these CTLs stimulated by END$^+$/Gal$^+$-MHCC97H/DC fusion cells were potently cytotoxic against MHCC97H (including END$^+$/Gal$^+$-MHCC97H and END$^-$/Gal$^-$-MHCC97H) and HUVEC cells. This is consistent with previously reported in the literature that the IL-12p70 secreted by mature DC could promote the secretion of IFN-γ from T cells and enhance the killing function of T cells[22]. The ability of αGal to promote antigen presentation in fusion cells may also be related to antigen cross-presentation, and further experiments are still needed.

In order to maximize the efficiency of cell adoptive immunotherapy, DCs must strongly present as many immunogenic antigens as possible (*e.g.*, tumor antigens, tumor vascular antigens, etc.) to T cells[23−25]. However, the current CAR-T cells can only target some known tumor antigens, not unknown others. Whereas, the CTLs induced by tumor/DC fusion cells can target the unknown antigens as well as known ones. Besides, our current strategy allows DCs to present not only more known and unknown tumor antigens, but also αGal and END to T cells *via* antigen cross-presentation. Therefore, it is regarded as a bifunctional tumor vaccine which can both target tumor cells and tumor neovascular endothelial cells. The hyperacute rejection against tumors induced by αGal extended to the neovascular endothelial cells of the tumor, which significantly enhanced the potency of CTLs against the entire tumor tissue. Based on the TCGA database, we analyzed the difference in the expression level of END between a variety of tumors and non-tumor tissues. The results showed that most tumors such as CHOL, ESCA, HNSC, KIRC, STAD, THCA, etc., had significantly different END expression levels from non-tumor tissues (Supporting Information Fig. S5A). Furthermore, we observed a marked difference in OS between high- and low-risk groups based on the risk score. The results showed that the survival time of HCC patients with high END expression was significantly shorter than that of patients with low expression (Fig. S5B). The anti-tumor effects against tumor blood vessels could suppress tumor and also inhibit metastasis by depriving its nutrition supply[26−28].

This study has certain limitation that the bifunctional tumor vaccine is not directly injected into tumor-bearing mice to observe its anti-tumor effect, and need to be explored in subsequent studies. This research used MHCC97H tumor as a representative to confirm the effectiveness of the vaccine. The further study will be carried out to verify the feasibility of the vaccine in lung cancer, breast cancer, ovarian cancer, etc. In summary, this work demonstrated a new strategy for cell-based vaccinations against tumors.

5. Conclusions

Our study revealed that DCs fused with MHCC97H cells and expressed both αGal and END, the resulting fusion cells were then used to activate CTLs. The activated T cells effectively inhibited tumor growth and prolonged survival of mice bearing human hepatomas, suggesting an effective clinical potential for this new cell-based vaccine.

Acknowledgments

Our sincere thanks to Prof. Peng Chen from Nanyang Technological University (Singapore) for his contribution to the revision. This work was supported, in part, by grants from the State Project for Essential Drug Research and Development (No. 2019ZX09301132, China), National Natural Science Foundation of China (Nos. 82060562 and 82072340), the Scientific and Technological Innovation Major Base of Guangxi (No. 2018-15-Z04, China), and Guangxi Key Research and Development Project (No. AB20117001, China), and Guangxi Natural Science Foundation (No. 2018JJA140524, China).

Author contributions

Jian He, Yu Huo and Zhikun Zhang designed and performed experiments, analyzed data, and wrote the paper. Xiuli Liu, Lan Li, Huixue Wang and Chao Tang performed some experiments. Pan

Wu, Qiaoying Chen and Yiqun Luo analyzed data. Wei Shi, Tao Wu, Yong Huang and Yongxiang Zhao provided assistance in the study. Lu Gan, Bing Wang and Liping Zhong initiated the study, organized, designed, and wrote the paper. All authors read and approved the final manuscript.

Conflicts of interest

The authors declare no conflicts of interest.

Appendix A. Supporting information

Supporting data to this article can be found online at https://doi.org/10.1016/j.apsb.2022.03.002.

References

1. Ferlay J, Soerjomataram I, Dikshit R, Eser S, Mathers C, Rebelo M, et al. Cancer incidence and mortality worldwide: sources, methods and major patterns in GLOBOCAN 2012. *Int J Cancer* 2015;**136**:E359−86.
2. Rimassa L, Personeni N, Czauderna C, Foerster F, Galle P. Systemic treatment of HCC in special populations. *J Hepatol* 2021;**74**:931−43.
3. Li S, Liu R, Pan Q, Wang G, Cheng D, Yang J, et al. *De novo* lipogenesis is elicited dramatically in human hepatocellular carcinoma especially in hepatitis C virus-induced hepatocellular carcinoma. *MedComm* 2020;**1**:178−87.
4. Vinanica N, Yong A, Wong D, Png YT, Seow SV, Imamura M, et al. Specific stimulation of T lymphocytes with erythropoietin for adoptive immunotherapy. *Blood* 2020;**135**:668−79.
5. Krishna S, Lowery FJ, Copeland AR, Bahadiroglu E, Mukherjee R, Jia L, et al. Stem-like CD8 T cells mediate response of adoptive cell immunotherapy against human cancer. *Science* 2020;**370**:1328−34.
6. Burbage M, Amigorena S. A dendritic cell multitasks to tackle cancer. *Nature* 2020;**584**:533−4.
7. He J, Zheng R, Zhang Z, Tan J, Zhou C, Zhang G, et al. Collagen I enhances the efficiency and anti-tumor activity of dendritic-tumor fusion cells. *OncoImmunology* 2017;**6**:e1361094.
8. Gammon JM, Jewell CM. Dendritic cell tracking and modulation. *Nat Mater* 2020;**19**:1134−5.
9. Liu WL, Zou MZ, Liu T, Zeng JY, Li X, Yu WY, et al. Cytomembrane nanovaccines show therapeutic effects by mimicking tumor cells and antigen presenting cells. *Nat Commun* 2019;**10**:3199−211.
10. Brown MC, Holl EK, Boczkowski D, Dobrikova E, Mosaheb M, Chandramohan V, et al. Cancer immunotherapy with recombinant poliovirus induces IFN-dominant activation of dendritic cells and tumor antigen-specific CTLs. *Sci Transl Med* 2017;**9**:e4220−50.
11. Kajihara M, Takakura K, Ohkusa T, Koido S. The impact of dendritic cell-tumor fusion cells on cancer vaccines—past progress and future strategies. *Immunotherapy* 2015;**7**:1111−22.
12. Bernth Jensen JM, Laursen NS, Jensen RK, Andersen GR, Jensenius JC, Sørensen UBS, et al. Complement activation by human IgG antibodies to galactose-α-1,3-galactose. *Immunology* 2020;**161**:66−79.
13. Springett GM. Novel pancreatic cancer vaccines could unleash the army within. *Cancer Control* 2014;**21**:242−6.
14. Tanemura M, Miyoshi E, Nagano H, Eguchi H, Matsunami K, Taniyama K, et al. Cancer immunotherapy for pancreatic cancer utilizing α-gal epitope/natural anti-Gal antibody reaction. *World J Gastroenterol* 2015;**21**:11396−410.
15. Yoshitomi H, Kobayashi S, Ohtsuka M, Kimura F, Shimizu H, Yoshidome H, et al. Specific expression of endoglin (CD105) in endothelial cells of intratumoral blood and lymphatic vessels in pancreatic cancer. *Pancreas* 2008;**37**:275−81.
16. Fujita K, Ewing CM, Chan DY, Mangold LA, Partin AW, Isaacs WB, et al. Endoglin (CD105) as a urinary and serum marker of prostate cancer. *Int J Cancer* 2009;**124**:664.
17. Schoonderwoerd MJA, Koops MFM, Angela RA, Koolmoes B, Toitou M, Paauwe M, et al. Targeting endoglin-expressing regulatory T cells in the tumor microenvironment enhances the effect of PD1 checkpoint inhibitor immunotherapy. *Clin Cancer Res* 2020;**26**:3831−42.
18. Wu HW, Sheard MA, Malvar J, Fernandez GE, DeClerck YA, Blavier L, et al. Anti-CD105 antibody eliminates tumor microenvironment cells and enhances anti-GD2 antibody immunotherapy of neuroblastoma with activated natural killer cells. *Clin Cancer Res* 2019;**25**:4761−74.
19. Duffy AG, Ma C, Ulahannan SV, Rahma OE, Makarova-Rusher O, Cao L, et al. Phase I and preliminary phase II study of TRC105 in combination with sorafenib in hepatocellular carcinoma. *Clin Cancer Res* 2017;**23**:4633−41.
20. Wang Z, Yin N, Zhang Z, Zhang Y, Zhang G, Chen W. Upregulation of T-cell immunoglobulin and mucin-domain containing-3 (Tim-3) in monocytes/macrophages associates with gastric cancer progression. *Immunol Invest* 2017;**46**:134−48.
21. Sianturi J, Manabe Y, Li HS, Chiu LT, Chang TC, Tokunaga K, et al. Development of α-Gal−antibody conjugates to increase immune response by recruiting natural antibodies. *Angew Chem Int Ed Engl* 2019;**58**:4526−30.
22. Wong KL, Tang LF, Lew FC, Wong HS, Chua YL, MacAry PA, Kemeny DM. CD44^{high} memory CD8 T cells synergize with CpG DNA to activate dendritic cell IL-12p70 production. *J Immunol* 2009;**183**:41−50.
23. Sabado RL, Balan S, Bhardwaj N. Dendritic cell-based immunotherapy. *Cell Res* 2017;**27**:74−95.
24. Burbage M, Amigorena S. A dendritic cell multitasks to tackle cancer. *Nature* 2020;**584**:533−4.
25. Wculek SK, Cueto FJ, Mujal AM, Melero I, Krummel MF, Sancho D. Dendritic cells in cancer immunology and immunotherapy. *Nat Rev Immunol* 2020;**20**:7−24.
26. Garris CS, Luke JJ. Dendritic cells, the T-cell-inflamed tumor microenvironment, and immunotherapy treatment response. *Clin Cancer Res* 2020;**26**:3901−7.
27. Palikuqi B, Nguyen DT, Li G, Schreiner R, Pellegata AF, Liu Y, et al. Adaptable haemodynamic endothelial cells for organogenesis and tumorigenesis. *Nature* 2020;**585**:426−32.
28. Lechertier T, Reynolds LE, Kim H, Pedrosa AR, Gómez -Escudero J, Muñoz -Félix JM, et al. Pericyte FAK negatively regulates Gas6/Axl signalling to suppress tumour angiogenesis and tumour growth. *Nat Commun* 2020;**11**:2810−24.